ACS APPLIED POLYMER MATERIALS

Article

Cite This: ACS Appl. Polym. Mater. 2019, 1, 369−380

pubs.acs.org/acsapm

Injectable Poly(oligoethylene glycol methacrylate)-Based Hydrogels Fabricated from Highly Branched Precursor Polymers: Controlling Gel Properties by Precursor Polymer Morphology

Ivan Urosev,[†] Helen Dorrington,[‡] Nicola Muzzin,[‡] Richard Alsop,[§] Emilia Bakaic,[†] Trevor Gilbert,[†] Maikel Rheinstädter,[§] and Todd Hoare*[,†,‡]

[†]School of Biomedical Engineering, McMaster University, 1280 Main Street W., Hamilton, Ontario L8S 4L7, Canada

[‡]Department of Chemical Engineering, McMaster University, 1280 Main Street W., Hamilton, Ontario L8S 4L7, Canada

[§]Department of Physics and Astronomy, McMaster University, 1280 Main Street W., Hamilton, Ontario L8S 4L7, Canada

Supporting Information

ABSTRACT: The physicochemical properties of injectable hydrogels are typically modified by altering the chemistry of the precursor polymer and/or the amount or type of cross-linker, both of which can lead to hydrogels with altered mechanics, swelling, degradation, and other key physical properties. Herein, we describe an alternative approach to tune the properties of injectable hydrogels (here, based on hydrazone cross-linked poly(oligoethylene glycol methacrylate), or POEGMA) by altering the architecture of the precursor polymers through branching. Hydrogels prepared using highly branched precursor polymers had nearly identical chemical compositions but exhibited markedly different physical properties relative to linear precursor hydrogels on which we have previously reported. Specifically, increasing the degree of branching resulted in increased degradation time and stiffness but decreased gelation time and gel swelling. The mechanical properties of highly branched hydrogels are relatively insensitive to the mass concentration of precursor polymer used to prepare the gels, in contrast to hydrogels prepared with linear precursors; furthermore, gels prepared from only highly branched precursors exhibit substantially prolonged degradation times compared to all-linear or linear−highly branched hydrogels. Overall, introducing branching in the precursor polymers is demonstrated to provide an alternate strategy to tune injectable hydrogel properties while decoupling otherwise coupled properties (e.g., polymer concentration and mechanics).

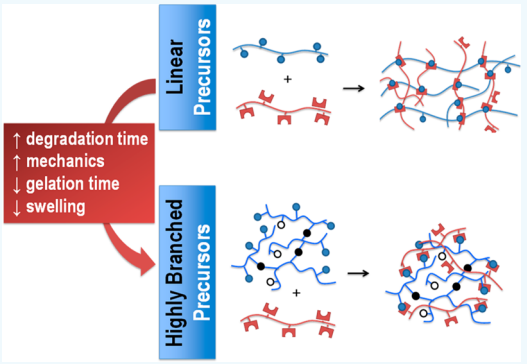

KEYWORDS: *highly branched polymers, hydrogel, in situ gelling, poly(oligoethylene glycol methacrylate), injectable*

INTRODUCTION

Hydrogels have attracted significant research interest in a biomedical context due to their structural, mechanical, and in some cases chemical similarity to the extracellular matrix (ECM) that forms the bulk of the cellular environment *in vivo*.[1−3] For maximum clinical applicability, injectable or *in situ* forming hydrogels prepared by exploiting either physical or chemical cross-linking strategies[4−8] are generally preferred to preformed gels, which often must be surgically implanted. A variety of *in situ* gelling hydrogels has been reported based on both synthetic and natural polymers, with synthetic polymers having particular advantages in terms of their highly controllable compositions and architectures[9,10] that enable more facile customization of hydrogel properties (i.e., stiffness, porosity, degradation rate, cell interactivity, etc.) to suit a particular application.[11,12] Poly(ethylene glycol) (PEG) and its derivatives have attracted particular attention due to the typically high tissue compatibility of PEG-based hydrogels.[13] However, because PEG is an uncharged and unreactive polymer with only chain-end functionality, minimal reactive sites are available for facilitating both functionalization and cross-linking.[14] As an alternative, poly(oligoethylene glycol methacrylate) (POEGMA) features PEG side chains of controllable lengths tethered to a methacrylate backbone that can be copolymerized with any compatible functional (meth)acrylate-based monomer to incorporate any desired number or type of functional groups into the polymer. In this manner, POEGMA-based polymers (and thus hydrogels comprised of these polymers) can be engineered to exhibit the same desirable properties of PEG (i.e., low nonspecific protein adsorption and host response) while being significantly easier to tune for specific target applications.[15]

Our group has devoted significant research attention to the development of *in situ* gelling hydrogels based on POEGMA

Received: November 12, 2018
Accepted: January 24, 2019
Published: January 24, 2019

DOI: 10.1021/acsapm.8b00085
ACS Appl. Polym. Mater. 2019, 1, 369−380

Scheme 1. Preparation of Injectable *in situ* Gelling Hydrogels from Highly Branched Hydrazide-Functionalized POEGMA and Linear Aldehyde-Functionalized POEGMA[a]

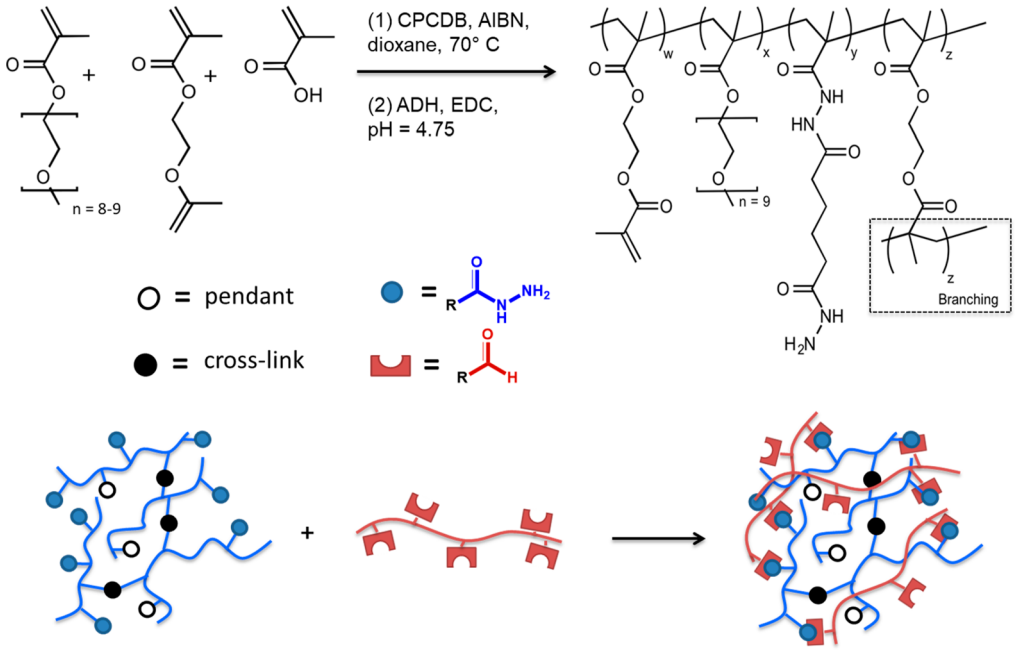

[a]See Supporting Information, Scheme S1 for corresponding chemistry for linear precursor polymers.

precursor polymers containing complementary hydrazide/aldehyde functional groups.[16] In follow-up work, we have shown that properties such as the stiffness, degradation rate, and gelation time of injectable POEGMA hydrogels can be chemically modulated by changing the degree of functionality of the precursor POEGMA polymers and/or the length of the PEG side chains of the constituent monomers,[17,18] enabling the fabrication of *in situ*-gelling hydrogels with a range of target properties. Most recently, we demonstrated that modifying only the structural properties (specifically, the molecular weight) of the precursor polymers can similarly enable precise tuning of gel properties.[19] This approach is particularly advantageous relative to other strategies in that it allows for a clear decoupling of the gel chemistry with the gel properties; for example, lowering the molecular weight of the precursor polymers resulted in gels with weaker mechanical properties but the exact same density of chemical cross-linking groups. Such capacity for chemistry-independent tuning of gel properties has substantial potential applications in terms of, for example, differentiating the effects of chemistry and mechanics on protein adsorption and/or cell responses to hydrogels, of particular importance in decoupling the roles of ECM in influencing stem cell differentiation.[20] However, given that the molecular weight of POEGMA-based precursor polymers can only be controlled effectively over a certain range, the scope of achievable gel properties using this approach was also limited.

Aside from molecular weight, significant changes in hydrogel properties can also be introduced by altering the morphology of the precursor polymers. Specific to PEG, multiarm PEG precursor polymers have been widely used to prepare hydrogels. Relative to linear precursor PEGs, multiarm PEGs provide substantially more reactive functional groups per precursor polymer while still maintaining a highly uniform internal structure, resulting in the formation of homogeneous network hydrogels with typically high strength.[21−24] Dendrimers prepared from a broader set of precursor polymers have been explored for a similar purpose, with their highly regulated branched structure offering key advantages in terms of promoting gel homogeneity and enhancing the overall cross-link density of the hydrogel.[25−27] However, both star-PEGs and dendrimers are synthetically demanding to prepare,[28] making them less attractive for bulk gel applications *in vivo*. Instead, highly branched polymers (HBPs), globular macromolecules with a highly internally branched nanostructure, have attracted significant attention recently.[25,29−31] The high peripheral functionality and functional group accessibility in HBPs (directly analogous to dendrimers) can promote higher cross-linking and drug loading as compared to analogous linear polymers.[25] HBPs based on free radical polymerizable monomers can also be prepared via "one-pot" methods without the need for multiple isolation and purification steps typical of dendrimer synthesis[32,33] and with tunable degrees of branching, a parameter that is typically invariable with dendrimers.[34]

Combining HBPs with tunable branching degrees with linear polymers or proteins has further been demonstrated to affect the stability, stiffness, functional group accessibility, and/or diffusion profile of a hydrogel.[28,35,36] As an example from a functionalization perspective, Hassan et al. showed extended cell viability and conserved cellular behavior (e.g., cytokine and growth factor secretion) of human adipose-derived stem cells (hADSCs) encapsulated in highly branched-PEG/linear hyaluronic acid (HA) hydrogels; the presence of many functional groups at the periphery of the highly branched polymers was essential for facilitating postpolymerization functionalization with proteins and other cell-signaling molecules.[37] As an example from a diffusion perspective, Liu et al. demonstrated effective slowing of protein release kinetics by exploiting the HBP-induced nanodomains within an injectable highly branched phosphoramidate/linear HA hydrogel.[38] As an example from the mechanical perspective, Lin et al.

DOI: 10.1021/acsapm.8b00085
ACS Appl. Polym. Mater. 2019, 1, 369−380

showed that the elastic modulus of hydrogels prepared from thermoreversible gels based on PEG and PNIPAM copolymers with block or star architectures was a strong function of the degree of branching.[39] Thus, combining well-defined HBPs with linear polymer precursor polymers offers clear potential to modulate the properties of *in situ*-gelling hydrogel systems. In particular, we hypothesize that using a prenetworked precursor polymer such as a highly branched polymer will allow multiscale control over the cross-link density of hydrogels (i.e., both within and between the highly branched polymers), enabling the decoupling of properties otherwise difficult to decouple in covalently cross-linked injectable hydrogels (e.g., polymer concentration and mechanics).

Herein, we describe the formation of *in situ*-gelling (via hydrazone chemistry) POEGMA hydrogels based on highly branched precursor polymers prepared with controlled degrees of branching by RAFT (reversible addition−fragmentation chain transfer) polymerization (Scheme 1, Scheme S-1). Relative to the conventional use of chain transfer agents to prepare highly branched polymers,[39] RAFT enables the synthesis of more controlled and more soluble highly branched polymers (including those based on POEMGA[40,41]); adjusting the temperature and RAFT agent concentration can effectively tune the size and branching degree of the final HBPs produced.[42] By leveraging such control, we observe that preparing *in situ*-gelling hydrogels using more highly branched building blocks leads to gels with stronger mechanics, slower degradation, and reduced swelling but similar biological properties compared to gels prepared with less branched building blocks. This result suggests that the use of highly branched precursor polymers is a useful approach for tuning the properties of injectable hydrogels by manipulating the structural morphology of the gel precursors but without substantially altering the chemistry.

EXPERIMENTAL SECTION

Materials. All chemicals were purchased from Sigma-Aldrich (Oakville, ON) unless otherwise indicated. Ethylene glycol dimethacrylate (EGDMA, 98%) was passed through a column of basic aluminum oxide (Sigma-Aldrich, type CG-20) to remove the methyl ether hydroquinone inhibitor prior to use. Oligo(ethylene glycol) methyl ether methacrylate ($OEGMA_{475}$, 95%) with an average molecular weight of 475 g mol^{-1} and methacrylic acid (MAA, 99%) were purified via passage over a column of basic aluminum oxide (type CG-20) to remove the methyl ether hydroquinone (MEHQ) and butylated hydroxytoluene (BHT) inhibitors. Azobis-(isobutyronitrile) (AIBN, 95%), 2-cyano-2-propyl 4-cyanobenzodithioate (CPCDB, 98%), adipic acid dihydrazide (ADH, Alfa Aesar, 98%), *N*′-ethyl-*N*-(3-(dimethylamino)propyl)-carbodiimide (EDC, Carbosynth, Compton CA, commercial grade), aminoacetaldehyde dimethyl acetal (ADA, 99%), *N*-hydroxysuccinimide (NHS, 98%), and *N*-cyclohexyl-2-aminoethanesulfonic acid (CHES, 99%) were used as received. 3T3 *Mus musculus* mouse cells were obtained from Cedarlane Laboratories (Burlington, ON). Dulbecco's modified Eagle's medium (DMEM, + glucose, + pyruvate), fetal bovine serum (FBS), penicillin/streptomycin (PS), and trypsin-EDTA were purchased from Invitrogen Canada (Burlington, ON). 1,4-Dioxane (reagent grade), dichloromethane (DCM, reagent grade), and diethyl ether (reagent grade) were purchased from Caledon Laboratory Chemicals (Georgetown, ON). Hydrochloric acid (HCl, 1 M) was received from LabChem Inc. (Pittsburgh, PA). Milli-Q grade distilled deionized water (DIW) was used for all experiments. Phosphate buffered saline (PBS) was prepared with the standard composition (10 mM phosphate buffer, 0.15 M total ionic strength, pH 7.4).

Methods. *Synthesis of Hydrazide-Functionalized Highly Branched/Linear POEGMA Polymers ($HBPn_H/LPn_H$).* A series of four highly branched POEGMA polymers was prepared with targeted degrees of branching of 15% ($HBP13.4_H$), 10% ($HBP9.2_H$), 5% ($HBP4.5_H$), and 0% ($LP0_H$); the number in each sample code indicates the measured DB for each polymer as per NMR, as described below. In a representative reaction ($HBP13.4_H$), $OEGMA_{475}$ (5 g), EGDMA (0.57 g), MAA (0.495 g), and AIBN (10.5 mg) were dissolved in 25 mL of 1,4-dioxane. The DB of the other HBPs prepared was varied by changing the mol % of EGDMA included in the reaction mixture from 0−15 mol % and correspondingly lowering the $OEGMA_{475}$ mole fraction to keep the total mole fraction of monomers in the reaction mixture constant; see Table 1 for full recipes. CPCDB (55.4 mg) was added to this solution, after which the solution was transferred to a sealed Schlenk flask, degassed via three freeze−pump−thaw cycles, and backfilled with N_2. The flask was then submerged in a preheated oil bath at 70 °C, and the mixture was allowed to react for 9 h. Samples were taken from the reaction at predetermined time intervals to facilitate analysis of conversion and molecular weight (MW) as a function of reaction time. After 9 h, the reaction was stopped by submerging the reaction vessel in an ice bath and exposing the reaction to air. Samples of the crude reaction mixture were collected as the final time point for the kinetics analysis, with the remaining mixture precipitated in 10× cold ethyl ether and used for further reactions. Note that an additional polymerization was conducted using a 10.5 h reaction time to attempt to increase the observed molecular weight; however, minimal benefits were observed as a result of the longer reaction time, and the sample was not further pursued (Table S1 and Supporting Figures S2 and S3).

Table 1. Synthesis Recipes for Highly Branched and Linear Hydrazide and Aldehyde-Functionalized POEGMA Polymers

polymer	[OEGMA]/[EGDMA]/[MAA] mole fraction	[monomer +EGDMA]/[CPCDB]/[AIBN] mole fraction	$M_{n,theory}$ (kDa)	DB_{theory} (%)
$HBP13.4_H$	55/15/30	100/1.12/0.33	26.9	15
$HBP9.2_H$	60/10/30	100/1.12/0.33	28.1	10
$HBP4.5_H$	65/5/30	100/1.12/0.33	29.3	5
$LP0_H$	70/30	100/1.12/0.33	30.5	0
$HBP15.4_A$	55/15/30	100/1.12/0.33	26.9	15
$LP0_A$	70/30	100/1.12/0.33	30.5	0

To prepare hydrazide-functionalized highly branched polymers, the remaining precipitate from the previous step was dissolved in 100 mL of deionized water to which ADH (10.03 g) was added. The pH of the solution was lowered to 4.75 by addition of 1 M HCl, after which 3.13 g of EDC was added to facilitate ADH functionalization of the −COOH groups from the MAA residues in the copolymer. The pH of the solution was maintained at 4.75 by the addition of 1 M HCl and 1 M NaOH as necessary for ∼4 h (or until the pH of the solution no longer changed). The reaction was subsequently allowed to stir overnight, after which the solution was transferred to a 3.5 kDa molecular weight cutoff regenerated cellulose membrane and dialyzed against deionized H_2O for 6 cycles (6 h each). The solution was then lyophilized to dryness to yield the final product, which resembled a clear wax. The product was dissolved at 250 mg mL^{-1} in 10 mM PBS and stored at 4 °C.

Synthesis of Aldehyde-Functionalized Highly Branched/Linear POEGMA Polymers ($HBPn_A/LPn_A$). Aldehyde-functionalized highly branched/linear POEGMA polymers were prepared to be used as the complementary polymer for preparation of injectable hydrogels with the highly branched/linear hydrazide-functionalized POEGMA polymers (Table 1). Aldehyde-functionalized POEGMA precursors were prepared using the same linear and highly branched polymer recipes outlined above up to the cold ether precipitation step; following, the precipitate was dissolved in 50 mL of dichloromethane, and 1.03 g of NHS and 1.38 g of EDC were added to the solution to

DOI: 10.1021/acsapm.8b00085
ACS Appl. Polym. Mater. 2019, 1, 369−380

NHS-activate the carboxyl groups of MAA residues in the precursor polymer. The reaction was allowed to proceed under stirring for 6 h, after which 1.41 g of ADA was added, and the solution was stirred for another 24 h. Dichloromethane was then removed by rotary evaporation, and the remaining polymer was dissolved in 150 mL of H_2O. Excess reactants were removed by 2 cycles of dialysis in a 3.5 kDa molecular weight cutoff regenerated cellulose membrane against DI H_2O (at least 6 h per cycle). The solution was then transferred to an Erlenmeyer flask, and 50 mL of 1 M HCl was added to hydrolyze the acetal groups of ADA to aldehydes. This reaction was allowed to stir for 48 h, and the resulting product was purified via 6 cycles of dialysis (at least 6 h per cycle). The mixture was subsequently lyophilized to dryness to yield the final product, which resembled a clear wax. The product was dissolved at a concentration of 250 mg mL^{-1} in 10 mM PBS and stored at 4 °C.

Characterization of Highly Branched and Linear POEGMA Polymers. Aqueous size exclusion chromatography (SEC) was performed on samples taken from the synthesis reactor at 2, 4, 6, and 9 h time points to track the polymerization kinetics of the linear and highly branched polymers. SEC was performed using a Waters 515 HPLC pump, a Waters 717 Plus autosampler, three Ultrahydrogel columns (30 cm × 7.8 mm i.d.; 0−3, 0−50, 2−300 kDa), and a Waters 2414 refractive index detector. The same mobile phase was used for all samples consisting of 0.5 M $NaNO_3$, 25 mM CHES buffer (pH 10.4), and 10 ppm of NaN_3 (flow rate = 0.8 mL min^{-1}). The elution time of the polymers was compared against linear PEG standards ranging from 106 to 584 kDa (Waters). ^1H NMR was also performed on these samples dissolved in d_6-DMSO using a 600 MHz AVANCE spectrometer (Bruker), enabling estimation of conversion as a function of time by comparing the vinyl peaks from unincorporated monomers against the peaks from the polymer backbone. The degree of branching was determined from the NMR data as described in the Supporting Information (Figure S3 and Equations S1−S4). Conductometric titrations were performed on the polymers following the synthesis reaction (to quantify MAA content of the base polymers) and following functionalization (to quantify the percentage conversion of MAA groups to hydrazide or aldehyde groups) using a Mantech automatic titrator, 0.1 M NaOH as the titrant, and a 1 mg/mL solution of polymer as the test sample. Cloud point temperatures were determined using a Variant Cary Bio 100 UV−vis spectrophotometer. A temperature ramp from 10 to 90 °C at a rate of 1 °C/min was performed on 5 mg/mL polymer solutions in 10 mM PBS, with measurements taken at 0.5 °C increments.

Preparation of Hydrogels. Hydrogels were prepared by pipetting equal volumes of the hydrazide- and aldehyde-functionalized polymer precursors dissolved in 20 wt % solutions (for the base hydrogels) up to 50 wt % solutions in 10 mM PBS into a preformed silicone rubber mold, mixing the precursor solutions together manually by repeated pipetting for 5−10 s, and sealing in a container (100% relative humidity) at room temperature to allow the precursor polymers to gel overnight (see Supporting Information, Figure S4 for a full visual description of the process). For swelling and degradation assays, the mold had a diameter of 9 mm and a volume of 250 μL; for rheology tests, the mold had a diameter of 12 mm and a volume of 400 μL. After extrusion into the appropriate mold, the polymer solution was mixed thoroughly and allowed to gel overnight at room temperature in a sealed container with 100% relative humidity. The gelation time for each of the hydrogels was determined by inversion of a 100 μL (total hydrogel volume) solution in a 2 mL Eppendorf tube (inverted every 30 s). Time of gelation was recorded once the gel had ceased flowing when inverted after 30 s (n = 3 repeats per gel).

Transparency. Thirty microliters of both hydrazide- and aldehyde-functionalized polymers were added to individual wells of a 96-well tissue culture plate (n = 4). Hydrogels were allowed to equilibrate overnight, during which the plate was sealed to prevent evaporation. The transmittance of each gel was subsequently measured at a wavelength of 595 nm using a VICTOR 3 plate reader. Measured transmittance values were compared to measurements of 10 mM PBS (equal volume) as a control. Results are reported as the average of four replicates, with the uncertainty representing the standard deviation of those replicates.

Residual Functional Group Assay. Hydrogels were prepared inside a 48-well tissue culture plate by sequentially adding 30 μL each of hydrazide- and aldehyde-functionalized polymer precursors at 20 wt % in 10 mM PBS and pipetting up and down rapidly to ensure the precursor polymer solutions were well-mixed. After allowing the gels to equilibrate overnight, 150 μL of hydrazide-reactive FITC (0.05 g/L in pH 8.5 carbonate buffer) was added in each well. After soaking overnight, all hydrogels were rinsed with fresh carbonate buffer (15 cycles x 5 min each) to remove any unreacted probe. After the rinse step, the fluorescence of both plates was measured using a VICTOR 3 plate reader (λ_{exc}= 488 nm and λ_{emi} = 535 nm, n = 3).

Rheology. Hydrogel discs were prepared as described above, removed from the molds, and mounted in a parallel plate geometry (12 mm diameter) on a Mach-1 Mechanical Tester (Biomomentum Inc., Laval, QC). All tests were performed at room temperature and in triplicate. The compressive moduli were determined by applying a 25% compression to the hydrogels at a rate of 3%/s (a degree of compression verified to lie within the linear viscoelastic range). Subsequent strain sweep and dynamic frequency sweep tests were performed on these precompressed hydrogel discs to determine the shear modulus; precompression was applied to ensure full contact between the somewhat irregular gel interface and the rheometry plates, recognizing that it is possible that the precompression used may slightly change the shear response versus a non prestrained sample. For this latter test, discs were first subjected to a strain sweep with amplitudes between 0.1 and 2.2° at 0.5 Hz (to identify the linear viscoelastic range) followed by a dynamic frequency sweep between 0.1 and 2.2 Hz at an amplitude within the linear viscoelastic region.

Small Angle Neutron Scattering (SANS). SANS experiments were conducted using the 30 m SANS NG3 at the NIST Center for Neutron Research (NCNR, Gaithersburg, MD). Sample-to-detector distances of 1 m (6 Å neutron wavelength), 4 m (6 Å neutron wavelength), and 13 m (6 Å neutron wavelength without a lens, 8.4 Å neutron wavelength with lens) were used for analysis. All precursors used for SANS experiments were dissolved to concentrations of 200 mg mL^{-1} in 10 mM PBS prepared in D_2O to provide contrast for neutron scattering. Gels were prepared for analysis according to previously described methods.[19] The scattering intensity ($I(q)$) of the charged POEGMA hydrogel networks was modeled based on Porod theory including stretch (eq 1).

$$I(q) = \frac{A}{q^n} + \left(\frac{1}{q^s}\right)\frac{C}{1 + (\xi q)^m} + B \quad (1)$$

Here, $I(q)$ is the scattering intensity, q is the scattering vector, A is the Porod scale, C is the Lorentzian scale, B is the background scattering, n is the Porod exponent (related to the local clustering of polymer chains), s is the stretch factor (where s = 0 describes unstretched (globular) chains and s = 1 describes fully stretched (cylindrical) chains), m is the Lorentzian exponent (typically ranging between m = 2 for good solvents and m = 4 for very poor solvents), and ξ is the Lorentzian screening length (related to the mesh size of the hydrogel).[39,40]

Swelling and Degradation Kinetics. Hydrogel discs were prepared as previously described. Once removed from molds, hydrogels were placed in preweighed cell culture inserts that were immediately weighed again to determine the initial hydrogel weight (W_0). Following, inserts were placed into a 12-well cell culture plate that contained 4 mL of either 10 mM PBS (for swelling assays) or 10 mM HCl (for accelerated degradation assays intended only to enable tracking of the relative degradability of different hydrogel compositions, not simulate physiological degradation times). At each sample point, the insets containing the hydrogels were removed from the plate; the excess PBS or HCl was removed by gently wicking the hydrogel surface, and the insets/hydrogels were weighed to determine W_t. The inserts/hydrogels were subsequently placed back in the plates with fresh PBS or HCl in the wells and incubated at the

DOI: 10.1021/acsapm.8b00085
ACS Appl. Polym. Mater. 2019, 1, 369−380

Table 2. Characterization of Highly Branched/Linear POEGMA Precursor Polymers[a]

polymer	DB_{theory} (%)	DB_{actual} (%)	M_n (kDa)	M_w (kDa)	$Đ$	X	MAA (mol %)	OEGMA (mol %)	EGDMA (mol %)
$HBP13.4_H$	15	13.4	22.6	51.3	2.27	0.83	26.1	56.9	17.0
$HBP9.2_H$	10	9.2	19.8	35.6	1.80	0.81	28.9	58.1	13.0
$HBP4.5_H$	5	4.5	15.6	21.2	1.36	0.81	25.8	66.7	7.5
$LP0_H$	0	0	13.9	16.7	1.20	0.67	29.6	70.4	0
$HBP15.4_A$	15	15.4	15.5	30.1	1.94	0.79	30.8	47.8	21.4
$LP0_A$	0	0	14.5	17.7	1.22	0.74	29.8	70.2	0

[a]DB = degree of branching; $Đ$ = dispersity; X = overall monomer conversion.

appropriate temperature until the next time point. The swelling ratio (SR) at any time point was calculated using eq 2:

$$SR = \frac{W_t}{W_0} \quad (2)$$

Swelling assays were performed at both room temperature (22 °C) and 37 °C, while degradation assays were performed only at 37 °C. Assays were considered complete when the hydrogel had been entirely degraded, as determined visually by the absence of any remaining residue within the inset; this time ranged from 1 h to 30 days based on the hydrogel and conditions being tested. Reported swelling ratios represent the average of four replicates, with error bars representing the standard deviation of those replicates.

In Vitro POEGMA Cytotoxicity Assay. The cytotoxicity of the highly branched/linear POEGMA polymers was screened using a resazurin fluorescence assay with 3T3 mouse fibroblasts. Fibroblasts were seeded into wells of a 96-well polystyrene tissue culture plate at concentrations of 10 000 cells/well and subsequently incubated for 24 h at 37 °C in DMEM supplemented with 10% FBS and 1% penicillin/streptomycin. Cells in experimental wells were then exposed to precursor POEGMA polymer solutions (dissolved in DMEM and sterilized via passage through a 0.2 μm Acrodisc filter) at concentrations ranging from 200 to 2000 μg mL^{-1} for 24 h at 37 °C. Following incubation with POEGMA polymers, both experimental and control wells were treated with a 10 μg/mL resazurin sodium salt solution and incubated at 37 °C for 4 h. Fluorescence readings from all wells were taken using a Biorad plate reader (model 550; λ_{exc} = 531 nm, λ_{emi} = 572 nm). The background fluorescence associated with the combination of media, resazurin, and POEGMA polymers at each relevant concentration was subtracted from the readings of the experimental wells to isolate the cell metabolite concentration. The fluorescence readings from experimental wells were compared against a cell-only control (no polymer) to determine relative cell viability. Reported cell viabilities represent an average of four replicate samples, while error bars represent one standard deviation from the mean of the measured cell viability percentages (n = 4).

Protein Adsorption. In a 96-well tissue culture plate, 30 μL of hydrazide- and aldehyde-functionalized polymers were sequentially added to each well and pipetted up and down rapidly to ensure that the pregel solutions were well-mixed. The plate was then sealed with Parafilm to prevent evaporation and incubated overnight to equilibrate the hydrogels. Subsequently, 60 μL of FITC-BSA at concentrations of 125, 250, and 500 μg mL^{-1} in 10 mM PBS was added to the wells. After incubation for 2 h at 37 °C, all wells were rinsed three times with fresh PBS to remove any unbound protein. The fluorescence of each well was measured using a VICTOR 3 plate reader, with the protein concentration calculated based on a calibration curve of FITC-BSA solution controls of the same concentrations (λ_{exc}= 488 nm and λ_{emi} = 535 nm; R^2 = 0.986). Reported average adsorption values represent the mean of four replicate samples, with the error bars representing the standard deviation of those four replicates.

RESULTS AND DISCUSSION

Characterization of Highly Branched and Linear POEGMA Polymers. A series of highly branched and linear POEGMA polymers (HBPX, where X indicates measured DB) was prepared with targeted degrees of branching ranging from 0 to 15%. RAFT was used to control the DB such that it did not exceed the gel point during polymerization, maintaining solubility for each of the highly branched polymers prepared. Table 2 shows the key properties of these precursor polymers.

The DB of the polymers closely matched the mol % of EGDMA included in the reaction, with each experimental product exhibiting a degree of branching at or just slightly below the theoretical target (Table 2). This slightly lower experimental branching degree is likely attributable either to the presence of pendant vinyl groups on cross-linkers that did not form a branch point with another polymer chain or to radicals that terminate prior to forming the cross-link.. EGDMA was also incorporated in slightly larger than, but close to, stoichiometric proportions. This difference may be related to slight variations in the copolymerization kinetics between $OEGMA_{475}$ and EGMDA and/or a higher transfer constant for CPCDB with respect to EGDMA than $OEGMA_{475}$, either of which is consistent with copolymerization kinetics studies on this system (Supporting Information, Figure S5).

MAA was incorporated nearly stoichiometrically into the HBPs, while functionalization of the $HBPn_H$ and $LP0_H$ polymers with hydrazide groups proceeded to ∼50% grafting of available MAA groups to yield functional polymers with ∼13−16 mol % of total monomer residues containing a hydrazide group (Table 3). No significant difference in functionalization efficiency was noted as a function of the DB. The functionalization of $HBP15.4_A$ with aldehyde groups proceeded with similar efficiency; however, the functionalization of $LP0_A$ was somewhat less efficient, with 33% conversion of MAA residues observed (corresponding to 10 mol % of total residues functionalized with aldehyde groups). We hypothesize the lower apparent conversion in the linear aldehyde polymer is related to the increased probability of aldehyde coupling (akin to formaldehyde polymerization[43]) in the linear polymer. In contrast, the more internally cross-linked structure of the

Table 3. Chemical Composition of Hydrazide and Aldehyde-Functionalized Highly Branched and Linear POEGMA Precursors

polymer	percent MAA residues functionalized (mol %)	percent total residues with cross-linkable group (mol %)
$HBP13.4_H$	50	13
$HBP9.2_H$	52	15
$HBP4.5_H$	54	14
$LP0_H$	53	16
$HBP15.4_A$	54	16
$LP0_A$	33	10

DOI: 10.1021/acsapm.8b00085
ACS Appl. Polym. Mater. 2019, 1, 369−380

highly branched polymer has significantly less chain mobility to sterically facilitate such linkages, preserving more of the grafted aldehydes in their uncoupled state. Regardless, the degree of functionalization in all cases is within the range of materials that have successfully gelled in past studies with all-linear precursor polymers.[16]

Kinetics and Extent of Gelation. A series of hydrogels was formed by mixing equal volumes of one of the $HBPX_H$ precursors with the LP_A precursor (both as 20% w/v solutions in 10 mM PBS) and allowing time for hydrazone cross-link formation. Hydrogels were also prepared by mixing the highest DB hydrazide and aldehyde-functionalized highly branched polymers ($HBP13.4_H$ and $HBP15.4_A$) to examine the effects of both precursor polymers being highly branched on gel properties. Gelation occurred with all combinations tested in time frames ranging from 10 to 35 min (Table 4).

Table 4. Gelation Times of Hydrogels Formed via Mixing of Highly Branched/Linear Hydrazide-Functionalized and Linear Aldehyde-Functionalized POEGMA Precursors[a]

hydrogel	$[P_{Hzd}]/[P_{Ald}]$ (mg mL^{-1})	gelation time (min)
$HBP13.4_H/LP0_A$	200/200	10
$HBP9.2_H/LP0_A$	200/200	15
$HBP4.5_H/LP0_A$	200/200	20
$LP0_H/LP0_A$	200/200	35
$HBP13.4_H/HBP15.4_A$	200/200	10

[a] $[P_{Hzd}]$ = concentration of hydrazide-functionalized precursor polymer; $[P_{Ald}]$ = concentration of aldehyde-functionalized precursor polymer

As the degree of branching of the hydrazide precursor polymer was decreased, the gelation time increased for hydrogels composed of polymers with the same degree of functionalization, consistent with literature results.[44] We attribute this result to the fact that gelation in any hydrogel system is driven by the formation of a sufficient number of cross-links between polymers to undergo a sol–gel transition.[38,39,45] An increase in the DB of a precursor polymer effectively increases the degree of cross-linking *internal* to that precursor HBP (i.e., more permanent EGDMA cross-links are formed inside the highly branched precursor polymers themselves); as such, a highly branched polymer with a higher DB will have to form fewer *external* hydrazone cross-links (i.e., cross-links between different highly branched precursor polymers) to reach the gel point, resulting in faster bulk gelation (Scheme 1). For the HBP-HBP gel, gelation occurs in the same time frame as the $HBP13.4_H/LP0_A$ highly branched–linear hydrogel, with the higher aldehyde content of $HBP15.4_A$ compared to $LP0_A$ offsetting the lower mobility of the reactive aldehyde groups and higher overlap concentration of $HBP15.4_A$ due to the compactness of the highly branched internal architecture.

The degree of cross-linking between hydrazide and aldehyde groups following the formation of each hydrogel was assessed via fluorescent labeling of residual functional hydrazide residues by hydrazide-reactive fluorescein isothiocyanate (FITC). Given that all of the hydrazide-functionalized precursor polymers have similar degrees of functionalization (Table 2), it was expected that each gel should contain a similar number of residual functional groups following gelation. Figure 1 indicates this is indeed the case, with no significant difference observed in the residual hydrazide group density as a function of the degree of branching of the hydrazide-functionalized HBP precursor polymer ($p > 0.05$ in any pairwise comparison). However, the all-highly branched precursor hydrogel contains significantly more unreacted hydrazide groups. This result is likely related to the significantly lower capacity of the sterically restricted highly branched aldehyde polymer to penetrate into the highly branched hydrazide polymer and access many of the available cross-linking groups, resulting in significantly lower *external* cross-link densities (albeit higher *internal* cross-link densities) relative to linear polymer-containing hydrogels and thus higher residual functional group contents.

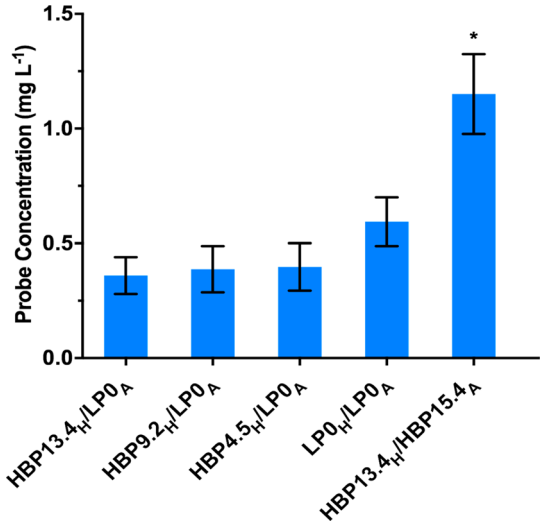

Figure 1. Calibrated fluorescence of hydrazide-reactive FITC bound to unreacted hydrazide functional groups in highly branched–linear and highly branched–highly branched POEGMA hydrogels. (*) Indicates $p < 0.05$ in a pairwise comparison with any other hydrogel tested. Error bars represent one standard deviation from the mean.

Rheology. The mechanical responses of hydrogels prepared with HBPs with different DB values were tested under both compressive and shear stress. Both types of stress were screened to identify whether the inherently higher mass density of a highly branched versus linear precursor polymer would disproportionally affect mechanics in response to shear in one dimension compared to others. Specifically, given the higher *internal* cross-linking coupled with the comparable or lower *external* (hydrazone) cross-linking of highly branched precursors (Figure 1), substantially different shear versus compressive moduli measurements may be anticipated for highly branched precursor hydrogels compared to linear precursor hydrogels. Table 5 summarizes the shear storage and compressive moduli of the gels tested as a function of precursor polymer DB.

The shear storage modulus (G') of highly branched–linear hydrogels increased in a nonlinear fashion as a function of the DB of the $HBPX_H$ precursors (Table 5), with a more than 6-fold increase in G' observed between gels prepared with the lowest DB $LP0_H$ and highest DB $HBP13.4_H$ precursors. This result is consistent with the increased *internal* cross-linking (due to higher EGDMA contents) and density of more highly branched precursor polymers which, when cross-linked together with a similar *external* cross-linking density (Figure 1), should result in gels with higher shear moduli. The compressive moduli followed the same general trends, exhibiting a nonlinear increase as a function of the DB of

DOI: 10.1021/acsapm.8b00085
ACS Appl. Polym. Mater. 2019, 1, 369–380

Table 5. Comparison of Shear Storage Modulus, Compressive Modulus, and Transmittance (at 595 nm) for Each Highly Branched−Linear and Highly Branched−Highly Branched Hydrogel Tested at 22°C

hydrogel composition	average shear storage modulus (kPa)	average compressive modulus (kPa)	normalized transmittance (%)[a]
$HBP13.4_H$/$LP0_A$	3.3 ± 0.2	18.3 ± 2.7	99.7
$HBP9.2_H$/$LP0_A$	1.7 ± 0.1	10.7 ± 1.9	99.1
$HBP4.5_H$/$LP0_A$	1.2 ± 0.1	9.0 ± 0.1	99.1
$LP0_H$/$LP0_A$	0.5 ± 0.1	7.5 ± 1.1	98.8
$HBP13.4_H$/$HBP15.4_A$	1.7 ± 0.2	9.9 ± 0.5	85.7

[a]Normalized transmittances are calculated by dividing the measured transmittance for the hydrogels by the measured transmittance for the same volume of PBS.

the precursor polymer. When both polymer precursors were highly branched, both the shear and compressive moduli decreased significantly. In this case, the increased density and *internal* (EGDMA) cross-linking density of the dual highly branched precursor gels is offset by the significantly lower *external* cross-link density achieved (as evidenced by higher number of residual functional groups in the all-highly branched hydrogel, Figure 1). We attribute this result to the combination of increased steric hindrance to interchain cross-linking (due to the higher density of the highly branched versus linear polymer) and reduced polymer flexibility (due to the internal branching of the highly branched polymer) leading to the formation of fewer cross-links between precursor polymers and thus weaker gels.

The absolute values of the moduli measured for these highly branched−linear combination gels are comparable to previously reported all-linear POEGMA hydrogels prepared at the same polymer concentration.[16,17] However, while the mechanics of these gels do lie within the range of some soft tissues of interest in the body,[46,47] they are on the lower end of relevant mechanics. To explore the scope of gel properties achievable with highly branched precursor polymers, the concentration of $HBP13.4_H$ (the highest modulus hydrogel among those tested) was varied from 20 wt % (the base case from Table 5) up to 50 wt %. The gelation time decreased from 10 min for the 20 wt % precursor solution to 3 min for the 50 wt % precursor solution. While this shorter gelation time was expected due to the higher polymer concentration, the observed change in gelation time is significantly less than that observed with linear polymers over a similar concentration range (20 min at 20 wt % but <1 min at 40 wt %). As such, the confined conformation of the highly branched building block significantly limits the kinetics of gelation irrespective of polymer concentration, a potential advantage in applications in which high weight content gels are desired but excessively fast gelation would introduce challenges with the delivery of the gel.

Similar impacts of the effect of the highly branched precursor polymer morphology are shown in the modulus changes as a function of $HPB13.4_H$ concentration in Table 6. As anticipated, the G' value increases as a function of the precursor polymer concentration. However, only a 1.6-fold increase in G' was observed over the full 20−50 wt % concentration range tested; in contrast, for linear polymer

Table 6. Concentration Effects on the Shear Storage Modulus of Highly Branched−Linear POEGMA Hydrogel ($HBP13.4_H$/$LP0_A$)

precursor concentration (w/v %)	average shear storage modulus (kPa)
20	3.3 ± 0.2
30	4.0 ± 0.1
40	4.2 ± 0.1
50	5.2 ± 0.7

precursor hydrogels tested over an even smaller concentration range (10−20 wt %), a 100-fold increase in G' was observed.[16] We anticipate that the faster gelation time of the concentrated precursor solutions will kinetically arrest the system at lower degrees of external cross-linking, with the relatively stiff highly branched building block minimizing the potential for additional external cross-linking. Given that mechanical tests primarily probe these external cross-links rather than the internal cross-link density of the highly branched polymers themselves, only small increases in the modulus values could be anticipated (as observed). In contrast, a gel prepared with all linear precursor polymers would retain significantly more conformational mobility, leading to higher ultimate cross-link densities. This interpretation is also consistent with the postgelation residual functional group labeling results in Figure 1, which showed decreased potential in the highly branched−highly branched gel networks to facilitate *external* cross-linking.

Internal Morphology. The transmittance values for each hydrogel prepared with one linear and one highly branched precursor polymer were comparable to the PBS-only reference (Table 5), with all gels appearing highly transparent and measured transmittance values ranging from 98.8 to 99.7% (i.e., within 1% over all highly branched−linear polymer combinations tested). Therefore, it is possible to tune the stiffness of highly branched hydrogels without sacrificing transparency, key for certain applications (e.g., ophthalmic). Hydrogels prepared with a gelling pair of highly branched precursors ($HBP13.4_H$/$HBP15.4_A$, Table 5) exhibited moderate opacity, consistent with the higher degree of mass clustering within the relatively conformationally immobile highly branched precursor units in this hydrogel.

Small angle neutron scattering analysis of highly branched hydrazide-linear aldehyde hydrogels as a function of the hydrazide polymer DB indicates significant trends in the key fitting parameters that relate to the internal microstructure of the gels. Table 7 shows the best-fit parameters for the Porod model with stretch (eq 1); see Supporting Information Figure S5 for the raw scattering data and best fit curves.

No large-scale heterogeneities were observed within any of the networks independent of DB, consistent with the high transparency of the networks; indeed, models built to model static inhomogeneities within hydrogels (e.g., the Ornstein-Zerinke/squared Lorentzian model)[48] provided poor fits for the experimental data. Thus, despite the highly branched structure of the hydrazide polymer building block, the resulting hydrogels are relatively homogeneous. The Porod exponent n is virtually unchanged as a function of DB, indicating that each highly branched polymer is solvated to a similar degree independent of the DB. The magnitude of n is also consistent with the dominance of mass fractals (i.e., a morphology between a Gaussian chain, $n = 2$, and a collapsed polymer coil, $n = 3$) in the scattering data, consistent with a highly branched structure. The Porod scale increases systematically with the DB

DOI: 10.1021/acsapm.8b00085
ACS Appl. Polym. Mater. 2019, 1, 369−380

Table 7. SANS Fitting Parameters for Highly Branched-Linear Hydrogels with Varying DB Precursor Polymers

hydrogel	Porod exponent (n)	Porod scale ($A \times 10^{-6}$)	stretch (s)	static correlation length (ξ) (Å)	Lorentzian exponent (m)	Lorentzian scale (C)	background
$HBP13.4_H/LP0_A$	2.77	3.37	0.32	8.6	4	0.92	0.19
$HBP9.2_H/LP0_A$	2.75	3.00	0.50	8.8	4	0.47	0.21
$HBP4.5_H/LP0_A$	2.77	2.75	0.13	9.2	4	1.42	0.23
$LP0_H/LP0_A$	2.80	2.50	0.03	9.4	4	1.80	0.20

of the hydrazide polymer, indicating an increased contribution of the fractal-like scattering component (i.e., the highly branched polymer) to the overall scattering profile at higher DB; concurrently, the Lorentzian scale (representing the scattering contributions of the fluid-like component of the gel) generally decreases as DB increases for the same reason. In tandem, the static correlation length (related to the mesh size of the main scattering unit, in this case the highly branched polymer component) decreases as a function of DB, consistent with the higher mass density within HBPs prepared with higher degree of branching. Finally, a significantly higher stretch term that represents nonrandom coil deformations within the constituent chains (predominantly the more flexible $LP0_A$ component of these highly branched−linear hydrogels) is required to fit HBP precursor hydrogels with higher DB values. This is consistent with the highly branched building blocks being more compact as the DB is increased, requiring increased "stretching" of the linear aldehyde-functionalized POEGMA polymers to link the highly branched precursor polymers together into a gel. Finally, while the Lorentzian exponent is higher than typical for hydrogels ($m = 4$ for all gels tested, typically representative of nonideal solvent interactions around helix-like associations)[49] the combination of the highly branched polymer structures and the branched structure of the $OEGMA_{475}$ monomer itself creates a highly nonidealized network structure relative to conventional hydrogels. Indeed, we have observed the need to use such high Lorentzian exponents in previous fits of POEGMA injectable hydrogels prepared from all-linear precursor polymers,[50] and the highly branched structure of the precursor polymers used herein would even further obscure the interpretation of this parameter relative to conventional hydrogel scattering theory.

Swelling and Degradation Kinetics. To assess the bulk physicochemical properties of the hydrogels as a function of the degree of branching of the precursor polymers, acid-catalyzed degradation and physiological swelling measurements were performed. Figure 2 shows the acid-catalyzed degradation kinetics of the hydrogels. We emphasize that acid-catalyzed conditions were not selected to mimic practical use conditions of the hydrogel but rather to accelerate the degradation assay to enable morphological comparisons over significantly shorter observation times; furthermore, our previous work with linear precursor injectable hydrogels has shown a correlation between the sequence of degradation times measured using the *in vitro* acid-catalyzed model and *in vivo* following subcutaneous injection, allowing the degradation times reported in Figure 2 to be at least semiquantitatively predictive of physiological degradation rates.[18,51]

Each degradation profile exhibits a similar general shape consisting of some initial swelling followed by rapid degradation, leading to a complete gel−sol transition within one day. The kinetic profiles observed are consistent with a diffusion-limited degradation process; as bonds are hydrolytically cleaved, more acid is able to penetrate the hydrogel

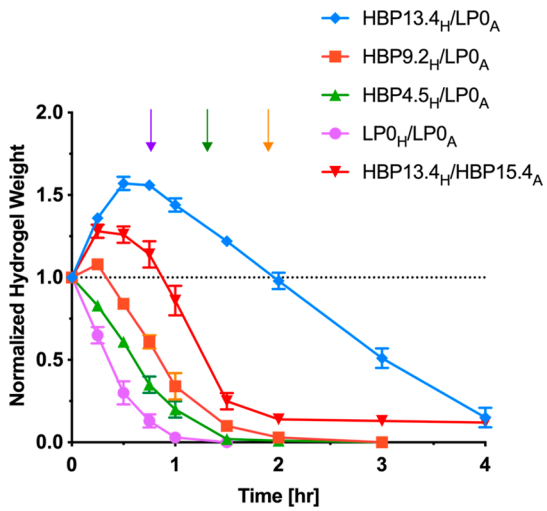

Figure 2. Degradation kinetics of highly branched POEGMA hydrogels in 10 mM HCl at 37 °C as a function of DB. Error bars for each measurement represent one standard deviation value from the mean ($n = 3$). Arrows indicate the time points at which the gel has degraded sufficiently to be completely washed out of the insets for each hydrogel tested. Lines are guides for the eye.

network to accelerate the degradation process. The degradation kinetics are inversely correlated with the DB of precursor polymers, as hydrogels prepared with higher DB precursor polymers degraded significantly slower. We attribute this result to the higher degree of *internal* cross-linking in precursor polymers prepared with higher DBs, reducing the rate at which the hydrogel swells, exposing fewer bonds to hydrolytic cleavage, and effectively prolonging the degradation time. The highly branched−highly branched precursor hydrogel $HBP13.4_H/HBP15.4_A$ degrades faster than the corresponding $HBP13.4_H/LP0_A$ hydrogel, consistent with the lower degree of *external* cross-linking observed in the $HBP13.4_H/HBP15.4_A$ hydrogel (Figure 1) and the very high lability of the hydrazone bond under the acidic degradation conditions.

The swelling responses for the same hydrogels in PBS were assessed at both physiological (37 °C) and room (~22 °C) temperature, with the results shown in Figure 3. At physiological temperature (Figure 3B), all of the gels followed a similar swelling profile consisting of a period of initial swelling followed by degradation until the solubilized gels washed out of the cell culture inserts. The profiles generally mirror the trends observed in the degradation assays in that slower rates of swelling and prolonged degradation times were observed for gels prepared with highly branched polymers with higher DB values; however, all the hydrogels swelled significantly more in PBS due to the deprotonation of the ~50 mol % residual carboxyl groups (not functionalized with hydrazide or aldehyde groups) on the precursor polymers at neutral pH that drives Donnan equilibrium-based swelling

DOI: 10.1021/acsapm.8b00085
ACS Appl. Polym. Mater. 2019, 1, 369−380

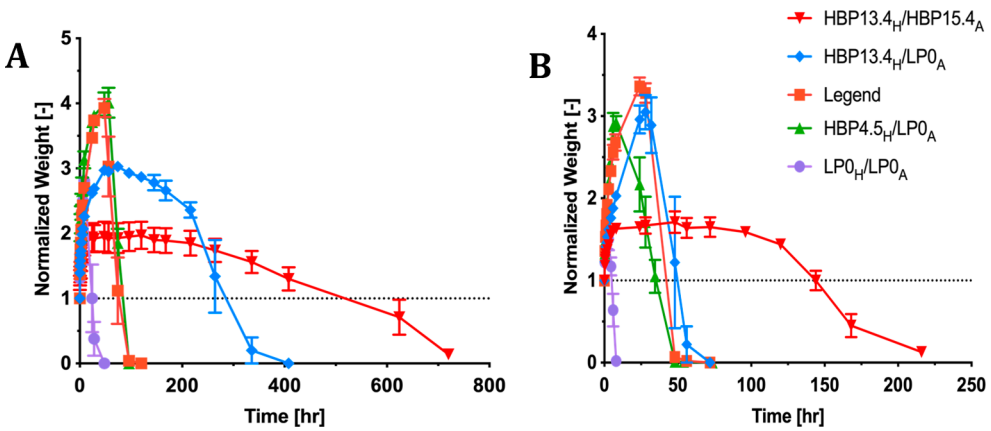

Figure 3. Swelling kinetics of hydrogels prepared in 10 mM PBS with highly branched POEGMA precursor polymers with varying degrees of branching at (A) 22 and (B) 37 °C. Error bars for each measurement represent one standard deviation value from the mean (n = 3). Lines are guides to the eye.

responses. Similar trends were noted at 22 °C (Figure 3A), although the times required for total degradation were roughly 3-fold longer than observed at 37 °C consistent with a conventional Arrhenius-like temperature dependence for the hydrolysis rate constants. However, the highly branched−highly branched hydrogel swells significantly less and degrades significantly slower than any of the highly branched−linear hydrogels tested at either test temperature. Again, this observation can be related to the much higher degree of *internal* cross-linking in the constituent precursor polymers, limiting the capacity of the gel to swell due to its reduced internal conformational mobility. At neutral pH, at which the hydrazone bond equilibrium favors bond formation, the significantly higher molecular weight of the highly branched polymers relative to the linear polymers (Table 2) requires simultaneous breaking of more hydrazone bonds to release a single precursor polymer unit in HBP13.4$_H$/HBP15.4$_A$ relative to HBP13.4$_H$/LP0$_A$ despite the lower number of *total* hydrazone cross-links that form in the all-HBP hydrogel (Figure 1).

Cell Viability Assay. The cytotoxicity of the highly branched and linear POEGMA polymers was determined using a resazurin assay conducted on 3T3 mouse fibroblasts. Figure 4 shows that none of the hydrazide-functionalized precursor polymers at any DB exhibited significant cytotoxicity, with >80% cell viability maintained relative to an untreated control even at concentrations of 2 mg/mL that are high for a closed *in vitro* assay.[16] These results are consistent with previous studies of linear POEGMA precursors with similar functionality,[52] suggesting that neither branching nor functionalization has a significant effect on the cytotoxicity of these materials. Moderate cytotoxicity was observed with the highly branched aldehyde polymer at concentrations >1 mg/mL, although cell viabilities are still relatively high (>60%) across the full concentration range. The higher surface density of aldehyde groups in highly branched materials relative to linear polymers (which do not show even this moderate cytotoxicity)[16,52] is likely the reason for this result, leading to a higher potential for protein cross-linking/denaturation. However, given the fast gelation times (Table 4) coupled with the slow degradation times (Figure 3) observed with highly branched aldehyde polymer-based gels, the practical concentration of HBP15.4$_A$ *in vivo* at any given time would be extremely low and unlikely to induce any significant toxicity response.

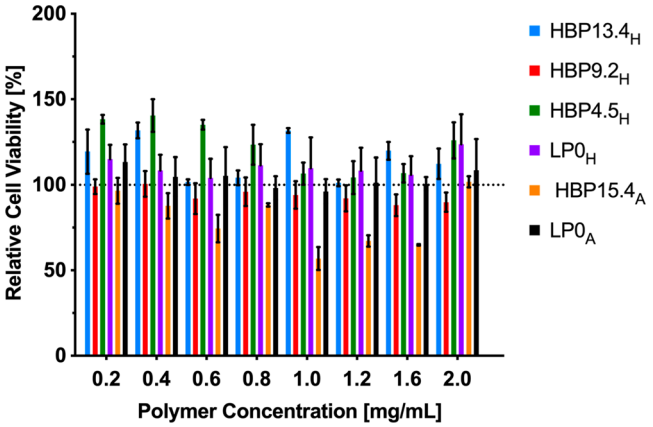

Figure 4. Relative viability of 3T3 mouse fibroblasts treated with HBP13.4$_H$ (blue), HBP9.2$_H$ (red), HBP4.5$_H$ (green), LP0$_H$ (purple), HBP15.4$_A$ (orange), and LP0$_A$ (black) for 24 h at concentrations ranging from 0.2 to 2 mg/mL. Error bars for each measurement represent one standard deviation from the mean of measured percent cell viability (n = 4).

Protein Uptake. The capacity of the highly branched precursor hydrogels to resist nonspecific protein adsorption/absorption was assayed by incubating the gels with fluorescently labeled BSA and tracking residual fluorescence, as shown in Figure 5. In general, introducing highly branched polymers into the hydrogels slightly increases the concentration of adsorbed protein to hydrogels, with statistically significant increases in protein adsorption noted between the all-linear hydrogel (LP0$_H$/LP0$_A$) and each of the highly branched−linear hydrogels (p < 0.05 for all pairwise comparisons at all BSA concentrations tested). Correspondingly, the highly branched−highly branched hydrogel adsorbed significantly more BSA than the highly branched−linear gels, consistent with the highly branched polymer content being effectively doubled in the all-highly branched gels relative to the highly branched−linear gels. However, the trend with DB in the highly branched−linear gels is not linear, with protein adsorption increasing from DB = 0 to 9.2 but then significantly decreasing at DB = 13.4. Note that this result was consistent for the higher molecular weight (longer reaction time) DB =

DOI: 10.1021/acsapm.8b00085
ACS Appl. Polym. Mater. 2019, 1, 369−380

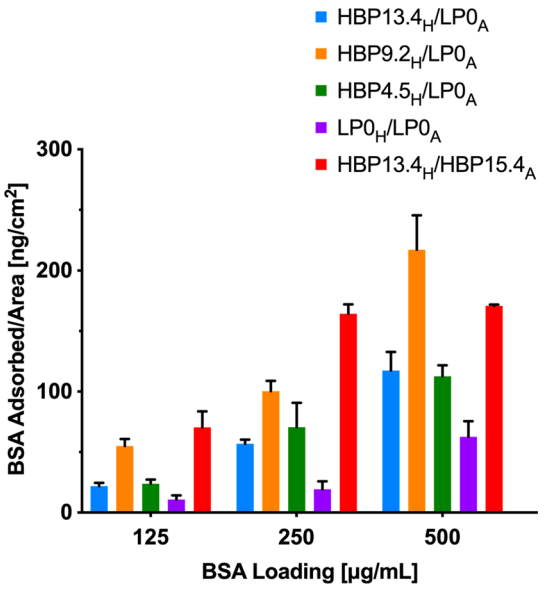

Figure 5. Uptake (adsorption + absorption) of FITC-BSA to highly branched POEGMA hydrogels (2 h incubation time 37 °C): $HBP13.4_H/LP0_A$ (blue); $HBP9.2_H/LP0_A$ (orange); $HBP4.5_H/LP0_A$ (green); $LP0_H/LP0_A$ (purple); $HBP13.4_H/HBP15.4_A$ (red). Error bars for each measurement represent one standard deviation value from the mean (n = 4).

12.6 gel tested (Supporting Information Figure S6), suggesting this observed maximum in protein binding is a real effect. This assay, as with others used for hydrogels, cannot explicitly differentiate between protein *absorption* into the bulk of the gel and protein *adsorption*; as such, we expect that the higher local mass density of hydrogels prepared with the highest DB (and thus densest) highly branched precursor polymers reduces BSA *absorption* to account for the lower measured values. The significantly lower degree of swelling observed with the DB = 13.4 hydrogel (Figure 3) further supports this interpretation, as lower influx of protein-containing buffer into the hydrogel would be observed upon equilibration relative to the other hydrogels tested. However, irrespective of branching, the total amount of adsorbed protein remained in the 10 to 100 ng/cm^2 range for similar BSA loading concentrations previously reported for PEG-grafted surfaces;[53−55] even at BSA concentrations of 0.5 mg/mL, the maximum adsorption amount of 217 ng/cm^2 was still significantly lower than many other reported polymeric biomaterials[56,57] despite the potential for dynamic Schiff base interactions between the proteins and any residual unreacted aldehydes within the gel. Indeed, this result is consistent with our previously reported linear POEGMA precursor-based hydrogels that similarly exhibited low protein adsorption *in vitro* coupled with only mild acute inflammatory responses and minimal if any chronic inflammatory responses *in vivo*,[18] despite the presence of a small fraction of residual aldehyde groups that can be of potential concern in terms of promoting inflammation. As such, these results confirm the potential of exploiting the key advantages of the highly branched precursor polymer structures (i.e., slower degradation, stronger mechanics, higher local mass density) without negatively influencing the biological performance of the materials.

In most previous studies, the key properties of synthetic injectable hydrogels (e.g., swelling, gelation times, mechanics, degradation, etc.) are engineered by changing either the polymers used to form the gel or the degree of functionality (and thus cross-linking potential) of those polymers.[13,16,52] However, this conventional approach inherently introduces chemical diversity into gels, making direct comparisons between the properties of different gels somewhat challenging as well as potentially introducing undesirable biological responses (i.e., for aldehyde-functionalized precursor polymers with higher functional group content, increased protein adsorption and cell interaction due to Schiff base formation with biomolecule/cell-tethered amines).[58,59] Alternatively, in this work, changes in bulk properties of injectable gels are instead driven by the compact architecture of the highly branched precursor polymers, with gel properties tuned simply by manipulating the degree of branching of the precursor polymers. Of particular note, several hydrogel properties such as the gelation time and the mass density can be significantly increased while only minimally affecting the shear and compressive moduli of the hydrogels (Table 6), in contrast to the highly correlated behavior of these properties in hydrogels prepared with all-linear precursor polymers.[16] Note that this correlation was also observed in our previous paper in which the molecular weight of the POEGMA precursors was altered to tune gel properties;[19] as such, the use of branching as a morphology-based control strategy for engineering gel properties appears to offer unique advantages. This capacity to decouple specific hydrogel properties has interesting potential implications in both drug delivery and cell encapsulation applications; for example, gels with higher internal cross-link densities (i.e., lower diffusion coefficients for controlled release and/or improved immunoisolation of allograft cells) could be prepared without significantly altering the bulk mechanics of the gel, important for mechanically matching an implant with the host tissue and/or mechanically signaling stem cell differentiation.[60] Furthermore, the potential to independently tune the cross-link density both *internally* within the highly branched precursor polymers (by manipulating the degree of branching and cross-linker content) and *externally* between the highly branched precursor polymers (by manipulating the amount of reactive functional group incorporated and/or the internal stiffness of the highly branched precursor polymers) provides multiple options for controlling the shear response under different geometries, offering a unique set of possibilities for engineering hydrogel properties not accessible using only conventional linear precursor polymers.

CONCLUSIONS

The use of highly branched POEGMA precursor polymers to form *in situ*-gelling hydrogels enables systematic tuning of hydrogel properties as a function of the degree of branching of the precursor polymers. Specifically, an increase in precursor polymer branching resulted in gels with higher stiffness, slower degradation under both physiological and acid-catalyzed conditions, faster gelation, and reduced swelling. Gels prepared from a combination of linear and highly branched precursors showed similar degrees of cross-linking and internal structures, while gels prepared from a combination of two highly branched precursors exhibited reduced overall external (i.e., interpolymer) cross-link density but significantly prolonged degradation times under physiological conditions. Collectively, these results demonstrate the potential of modifying polymer architecture for the design of highly tunable injectable hydrogels, particularly in cases where decoupling of chemistry and mechanics (i.e., interpreting stem cell responses to

DOI: 10.1021/acsapm.8b00085
ACS Appl. Polym. Mater. 2019, 1, 369−380

hydrogel biomaterials) and/or mass concentration and mechanics (i.e., controlled drug delivery vehicles) is desirable.

■ ASSOCIATED CONTENT

Supporting Information

The Supporting Information is available free of charge on the ACS Publications website at DOI: 10.1021/acsapm.8b00085.

Synthetic schemes for fabricating the linear and highly branched functional polymers, details on the chemical characterization of the highly branched polymers, data on the effect of polymerization time on highly branched polymer composition, representative photographs of the *in situ* gelation process, polymerization kinetics related to the production of highly branched polymers, raw small angle neutron scattering data on the highly branched injectable hydrogels, and protein uptake data on the highly branched injectable hydrogels (PDF)

■ AUTHOR INFORMATION

Corresponding Author

*E-mail: hoaretr@mcmaster.ca.

ORCID

Richard Alsop: 0000-0003-0563-0063
Maikel Rheinstädter: 0000-0002-0558-7475
Todd Hoare: 0000-0002-5698-8463

Notes

The authors declare no competing financial interest.

■ ACKNOWLEDGMENTS

The Natural Sciences and Engineering Research Council of Canada (NSERC, Discovery Grant RGPIN-356609 and Strategic Project Grant STPGP 447372-13) is gratefully acknowledged for financial support. This work utilized facilities supported in part by the National Science Foundation under Agreement DMR-0944772. We acknowledge the support of the National Institute of Standards and Technology, US Department of Commerce, in providing the neutron facilities used in this work.

■ REFERENCES

(1) Geckil, H.; Xu, F.; Zhang, X. H.; Moon, S.; Demirci, U. Engineering Hydrogels as Extracellular Matrix Mimics. *Nanomedicine* **2010**, *5*, 469−484.

(2) Rowley, J. A.; Madlambayan, G.; Mooney, D. J. Alginate Hydrogels as Synthetic Extracellular Matrix Materials. *Biomaterials* **1999**, *20*, 45−53.

(3) Tibbitt, M. W.; Anseth, K. S. Hydrogels as Extracellular Matrix Mimics for 3D Cell Culture. *Biotechnol. Bioeng.* **2009**, *103*, 655−663.

(4) Yu, L.; Ding, J. D. Injectable Hydrogels as Unique Biomedical Materials. *Chem. Soc. Rev.* **2008**, *37*, 1473−1481.

(5) Li, Y. L.; Rodrigues, J.; Tomas, H. Injectable and Biodegradable Hydrogels: Gelation, Biodegradation and Biomedical Applications. *Chem. Soc. Rev.* **2012**, *41*, 2193−2221.

(6) Kretlow, J. D.; Klouda, L.; Mikos, A. G. Injectable Matrices and Scaffolds for Drug Delivery in Tissue Engineering. *Adv. Drug Delivery Rev.* **2007**, *59*, 263−273.

(7) Ifkovits, J. L.; Burdick, J. A. Review: Photopolymerizable and Degradable Biomaterials for Tissue Engineering Applications. *Tissue Eng.* **2007**, *13*, 2369−2385.

(8) Patenaude, M.; Smeets, N. M. B.; Hoare, T. Designing Injectable, Covalently Cross-Linked Hydrogels for Biomedical Applications. *Macromol. Rapid Commun.* **2014**, *35*, 598−617.

(9) Hoffman, A. S. Hydrogels for Biomedical Applications. *Adv. Drug Delivery Rev.* **2012**, *64*, 18−23.

(10) Qiu, L. Y.; Bae, Y. H. Polymer Architecture and Drug Delivery. *Pharm. Res.* **2006**, *23*, 1−30.

(11) Nair, L. S.; Laurencin, C. T. Biodegradable Polymers as Biomaterials. *Prog. Polym. Sci.* **2007**, *32*, 762−798.

(12) Seliktar, D. Designing Cell-Compatible Hydrogels for Biomedical Applications. *Science* **2012**, *336*, 1124.

(13) Bakaic, E.; Smeets, N. M. B.; Hoare, T. Injectable Hydrogels Based on Poly(Ethylene Glycol) and Derivatives as Functional Biomaterials. *RSC Adv.* **2015**, *5*, 35469−35486.

(14) Hu, Z. B.; Cai, T.; Chi, C. L. Thermoresponsive Oligo-(Ethylene Glycol)-Methacrylate- Based Polymers and Microgels. *Soft Matter* **2010**, *6*, 2115−2123.

(15) Lutz, J.-F.; Andrieu, J.; Üzgün, S.; Rudolph, C.; Agarwal, S. Biocompatible, Thermoresponsive, and Biodegradable: Simple Preparation of "All-in-One" Biorelevant Polymers. *Macromolecules* **2007**, *40*, 8540−8543.

(16) Smeets, N. M. B.; Bakaic, E.; Patenaude, M.; Hoare, T. Injectable and Tunable Poly(Ethylene Glycol) Analogue Hydrogels Based on Poly(Oligoethylene Glycol Methacrylate). *Chem. Commun.* **2014**, *50*, 3306−3309.

(17) Bakaic, E.; Smeets, N. M. B.; Dorrington, H.; Hoare, T. "Off-the-Shelf" Thermoresponsive Hydrogel Design: Tuning Hydrogel Properties by Mixing Precursor Polymers with Different Lower-Critical Solution Temperatures. *RSC Adv.* **2015**, *5*, 33364−33376.

(18) Smeets, N. M.; Bakaic, E.; Patenaude, M.; Hoare, T. Injectable Poly(Oligoethylene Glycol Methacrylate)-Based Hydrogels with Tunable Phase Transition Behaviours: Physicochemical and Biological Responses. *Acta Biomater.* **2014**, *10*, 4143−55.

(19) Urosev, I.; Bakaic, E.; Alsop, R. J.; Rheinstadter, M. C.; Hoare, T. Tuning the Properties of Injectable Poly(Oligoethylene Glycol Methacrylate) Hydrogels by Controlling Precursor Polymer Molecular Weight. *J. Mater. Chem. B* **2016**, *4*, 6541−6551.

(20) Alakpa, E. V.; Jayawarna, V.; Lampel, A.; Burgess; West, C. C.; Bakker, S. C. J.; Roy, S.; Javid, N.; Fleming, S.; Lamprou, D. A.; Yang, J.; Miller, A.; Urquhart, A. J.; Frederix, P. W. J. M.; Hunt, N. T.; Péault, B.; Ulijn, R. V.; Dalby, M. J. Tunable Supramolecular Hydrogels for Selection of Lineage-Guiding Metabolites in Stem Cell Cultures. *Chem.* **2016**, *1*, 298−319.

(21) Nagahama, K.; Ouchi, T.; Ohya, Y. Temperature-Induced Hydrogels through Self-Assembly of Cholesterol-Substituted Star PEG-b-PLLA Copolymers: An Injectable Scaffold for Tissue Engineering. *Adv. Funct. Mater.* **2008**, *18*, 1220−1231.

(22) Tan, H.; DeFail, A. J.; Rubin, J. P.; Chu, C. R.; Marra, K. G. Novel Multiarm PEG-Based Hydrogels for Tissue Engineering. *J. Biomed. Mater. Res., Part A* **2009**, *92*, 979−987.

(23) Wang, J. Q.; Zhang, F. J.; Tsang, W. P.; Wan, C.; Wu, C. Fabrication of Injectable High Strength Hydrogel Based on 4-Arm Star PEG for Cartilage Tissue Engineering. *Biomaterials* **2017**, *120*, 11−21.

(24) Rose, J. C.; Camara-Torres, M.; Rahimi, K.; Kohler, J.; Moller, M.; De Laporte, L. Nerve Cells Decide to Orient inside an Injectable Hydrogel with Minimal Structural Guidance. *Nano Lett.* **2017**, *17*, 3782−3791.

(25) Mintzer, M. A.; Grinstaff, M. W. Biomedical Applications of Dendrimers: A Tutorial. *Chem. Soc. Rev.* **2011**, *40*, 173−190.

(26) Wang, J.; He, H.; Cooper, R. C.; Yang, H. In Situ-Forming Polyamidoamine Dendrimer Hydrogels with Tunable Properties Prepared via Aza-Michael Addition Reaction. *ACS Appl. Mater. Interfaces* **2017**, *9*, 10494−10503.

(27) Yang, H.; Tyagi, P.; Kadam, R. S.; Holden, C. A.; Kompella, U. B. Hybrid Dendrimer Hydrogel/PLGA Nanoparticle Platform Sustains Drug Delivery for One Week and Antiglaucoma Effects for Four Days Following One-Time Topical Administration. *ACS Nano* **2012**, *6*, 7595−7606.

(28) A, S.; Xu, Q.; Zhou, D.; Gao, Y.; Vasquez, J. M.; Greiser, U.; Wang, W.; Liu, W.; Wang, W. Hyperbranched PEG-Based Multi-NHS

Polymer and Bioconjugation with BSA. *Polym. Chem.* **2017**, *8*, 1283−1287.
(29) Dong, Y.; Saeed, A.; Hassan, W.; Tai, H.; Pandit, A.; Wang, W. Thiol-Ene Clickable PEG Based Thermoresponsive Hyperbranched Copolymer for in Situ Crosslinking Hybrid Hydrogel. *J. Tissue Eng. Regen M* **2012**, *6*, 190−191.
(30) Wang, D.; Jin, Y.; Zhu, X.; Yan, D. Synthesis and Applications of Stimuli-Responsive Hyperbranched Polymers. *Prog. Polym. Sci.* **2017**, *64*, 114−153.
(31) Joshi, N.; Grinstaff, M. Applications of Dendrimers in Tissue Engineering. *Curr. Top. Med. Chem.* **2008**, *8*, 1225−1236.
(32) Walter, M. V.; Malkoch, M. Simplifying the Synthesis of Dendrimers: Accelerated Approaches. *Chem. Soc. Rev.* **2012**, *41*, 4593−4609.
(33) Zhao, T.; Zheng, Y.; Poly, J.; Wang, W. Controlled Multi-Vinyl Monomer Homopolymerization through Vinyl Oligomer Combination as a Universal Approach to Hyperbranched Architectures. *Nat. Commun.* **2013**, *4*, 1873.
(34) Jin, H. B.; Huang, W.; Zhu, X. Y.; Zhou, Y. F.; Yan, D. Y. Biocompatible or Biodegradable Hyperbranched Polymers: From Self-Assembly to Cytomimetic Applications. *Chem. Soc. Rev.* **2012**, *41*, 5986−5997.
(35) Desai, P. N.; Yuan, Q.; Yang, H. Synthesis and Characterization of Photocurable Polyamidoamine Dendrimer Hydrogels as a Versatile Platform for Tissue Engineering and Drug Delivery. *Biomacromolecules* **2010**, *11*, 666−673.
(36) Xu, Q.; Venet, M.; Wang, W.; Creagh-Flynn, J.; Wang, X.; Li, X.; Gao, Y.; Zhou, D.; Zeng, M.; Lara-Sáez, I.; A, S.; Tai, H.; Wang, W. Versatile Hyperbranched Poly(B-Hydrazide Ester) Macromers as Injectable Antioxidative Hydrogels. *ACS Appl. Mater. Interfaces* **2018**, *10*, 39494−39504.
(37) Hassan, W.; Dong, Y.; Wang, W. Encapsulation and 3D Culture of Human Adipose-Derived Stem Cells in an in-Situ Crosslinked Hybrid Hydrogel Composed of PEG-Based Hyperbranched Copolymer and Hyaluronic Acid. *Stem Cell Res. Ther.* **2013**, *4*, 32.
(38) Liu, Y. H.; Zhang, F. H.; Ru, Y. Y. Hyperbranched Phosphoramidate-Hyaluronan Hybrid: A Reduction-Sensitive Injectable Hydrogel for Controlled Protein Release. *Carbohydr. Polym.* **2015**, *117*, 304−311.
(39) Gao, C.; Yan, D. Hyperbranched Polymers: From Synthesis to Applications. *Prog. Polym. Sci.* **2004**, *29*, 183−275.
(40) Dong, Y. X.; Saeed, A. O.; Hassan, W.; Keigher, C.; Zheng, Y.; Tai, H. Y.; Pandit, A.; Wang, W. X. "One-Step" Preparation of Thiol-Ene Clickable PEG-Based Thermoresponsive Hyperbranched Copolymer for in Situ Crosslinking Hybrid Hydrogel. *Macromol. Rapid Commun.* **2012**, *33*, 120−126.
(41) Luzon, M.; Boyer, C.; Peinado, C.; Corrales, T.; Whittaker, M.; Tao, L.; Davis, T. P. Water-Soluble, Thermoresponsive, Hyperbranched Copolymers Based on PEG-Methacrylates: Synthesis, Characterization, and LCST Behavior. *J. Polym. Sci., Part A: Polym. Chem.* **2010**, *48*, 2783−2792.
(42) Vogt, A. P.; Sumerlin, B. S. Tuning the Temperature Response of Branched Poly(N-Isopropylacrylamide) Prepared by Raft Polymerization. *Macromolecules* **2008**, *41*, 7368−7373.
(43) Vogl, O. Addition Polymers of Aldehydes. *J. Polym. Sci., Part A: Polym. Chem.* **2000**, *38*, 2293−2299.
(44) Kim, J.; Kong, Y. P.; Niedzielski, S. M.; Singh, R. K.; Putnam, A. J.; Shikanov, A. Characterization of the Crosslinking Kinetics of Multi-Arm Poly(Ethylene Glycol) Hydrogels Formed Via Michael-Type Addition. *Soft Matter* **2016**, *12*, 2076−2085.
(45) Ganji, F.; Abdekhodaie, M. J.; Ramazani, A. Gelation Time and Degradation Rate of Chitosan-Based Injectable Hydrogel. *J. Sol-Gel Sci. Technol.* **2007**, *42*, 47−53.
(46) Fung, Y. C. *Biomechanics: Mechanical Properties of Living Tissues*; Springer-Verlag: New York, 1981; p xii, 433.
(47) Griffin, M.; Premakumar, Y.; Seifalian, A.; Butler, P. E.; Szarko, M. Biomechanical Characterization of Human Soft Tissues Using Indentation and Tensile Testing. *J. Visualized Exp.* **2016**, 54872.
(48) Shibayama, M. Small-Angle Neutron Scattering on Polymer Gels: Phase Behavior, Inhomogeneities and Deformation Mechanisms. *Polym. J.* **2011**, *43*, 18−34.
(49) Hammouda, B.; Worcester, D. The Denaturation Transition of DNA in Mixed Solvents. *Biophys. J.* **2006**, *91*, 2237−2242.
(50) Bakaic, E.; Smeets, N. M. B.; Barrigar, O.; Alsop, R.; Rheinstadter, M. C.; Hoare, T. Ph-Ionizable in Situ Gelling Poly(Oligo Ethylene Glycol Methacrylate)-Based Hydrogels: The Role of Internal Network Structures in Controlling Macroscopic Properties. *Macromolecules* **2017**, *50*, 7687−7698.
(51) Bakaic, E.; Smeets, N. M. B.; Badv, M.; Dodd, M.; Barrigar, O.; Siebers, E.; Lawlor, M.; Sheardown, H.; Hoare, T. Injectable and Degradable Poly(Oligoethylene Glycol Methacrylate) Hydrogels with Tunable Charge Densities as Adhesive Peptide-Free Cell Scaffolds. *ACS Biomater. Sci. Eng.* **2018**, *4*, 3713−3725.
(52) Smeets, N. M. B.; Bakaic, E.; Patenaude, M.; Hoare, T. Injectable Poly(Oligoethylene Glycol Methacrylate)-Based Hydrogels with Tunable Phase Transition Behaviours: Physicochemical and Biological Responses. *Acta Biomater.* **2014**, *10*, 4143−4155.
(53) Farrell, M.; Beaudoin, S. Surface Forces and Protein Adsorption on Dextran- and Polyethylene Glycol-Modified Polydimethylsiloxane. *Colloids Surf., B* **2010**, *81*, 468−475.
(54) Jain, J. P.; Kumar, N. Self Assembly of Amphiphilic (PEG)(3)-PLA Copolymer as Polymersomes: Preparation, Characterization, and Their Evaluation as Drug Carrier. *Biomacromolecules* **2010**, *11*, 1027−1035.
(55) Weinman, C. J.; Gunari, N.; Krishnan, S.; Dong, R.; Paik, M. Y.; Sohn, K. E.; Walker, G. C.; Kramer, E. J.; Fischer, D. A.; Ober, C. K. Protein Adsorption Resistance of Anti-Biofouling Block Copolymers Containing Amphiphilic Side Chains. *Soft Matter* **2010**, *6*, 3237−3243.
(56) Roach, P.; Farrar, D.; Perry, C. C. Surface Tailoring for Controlled Protein Adsorption: Effect of Topography at the Nanometer Scale and Chemistry. *J. Am. Chem. Soc.* **2006**, *128*, 3939−3945.
(57) Tanaka, M.; Motomura, T.; Kawada, M.; Anzai, T.; Kasori, Y.; Shiroya, T.; Shimura, K.; Onishi, M.; Mochizuki, A. Blood Compatible Aspects of Poly(2-Methoxyethylacrylate) (PMEA) - Relationship between Protein Adsorption and Platelet Adhesion on PMEA Surface. *Biomaterials* **2000**, *21*, 1471−1481.
(58) Balakrishnan, B.; Mohanty, M.; Umashankar, P. R.; Jayakrishnan, A. Evaluation of an in Situ Forming Hydrogel Wound Dressing Based on Oxidized Alginate and Gelatin. *Biomaterials* **2005**, *26*, 6335−6342.
(59) Christensen, H. N. Three Schiff Base Types Formed by Amino Acids, Peptides and Proteins with Pyridoxal and Pyridoxal-5-Phosphate1. *J. Am. Chem. Soc.* **1958**, *80*, 99−105.
(60) Engler, A. J.; Sen, S.; Sweeney, H. L.; Discher, D. E. Matrix Elasticity Directs Stem Cell Lineage Specification. *Cell* **2006**, *126*, 677−689.

DOI: 10.1021/acsapm.8b00085
ACS Appl. Polym. Mater. 2019, 1, 369−380